

The SOPHIE spectrograph: design and technical key-points for high throughput and high stability

S. Perruchot^a, D. Kohler^a, F. Bouchy^b, Y. Richaud^a, P. Richaud^a, G. Moreaux^c, M. Merzougui^a, R. Sottile^a, L. Hill^a, G. Knispel^a, X. Regal^a, J.-P. Meunier^a, S. Ilovaisky^a, H. Le Coroller^a, D. Gillet^a, J. Schmitt^a, F. Pepe^d, M. Fleury^d, D. Sosnowska^d, P. Vors^a, D. Mégevand^d, P.E. Blanc^a, C. Carol^a, A. Point^a, A. Laloge^a, J.-C. Brunel^a

^aCNRS – Observatoire de Haute-Provence, F-04870 St-Michel-l'Observatoire;

^bCNRS – Institut D'astrophysique de Paris, 98bis bd Arago F-75014 Paris;

^cCNRS – Laboratoire d'astrophysique de Marseille, Pôle de l'Étoile Site de Château-Gombert, 38, rue Frédéric Joliot-Curie F-13388 Marseille cedex 13;

^dObservatoire de Genève, Université de Genève, 51 Chemin des Maillettes, 1290 Sauverny, Switzerland

Presented at SPIE "Astronomical Telescopes and Instrumentation 2008"
Marseille, June 23-28, 2008

ABSTRACT

SOPHIE is a new fiber-fed echelle spectrograph in operation since October 2006 at the 1.93-m telescope of Observatoire de Haute-Provence. Benefiting from experience acquired on HARPS (3.6-m ESO), SOPHIE was designed to obtain accurate radial velocities (~ 3 m/s over several months) with much higher optical throughput than ELODIE (by a factor of 10). These enhanced capabilities have actually been achieved and have proved invaluable in asteroseismology and exoplanetology. We present here the optical concept, a double-pass Schmidt echelle spectrograph associated with a high efficiency coupling fiber system, and including simultaneous wavelength calibration. Stability of the projected spectrum has been obtained by the encapsulation of the dispersive components in a constant pressure tank. The main characteristics of the instrument are described. We also give some technical details used in reaching this high level of performance.

Keywords: Instrumentation, optical design, spectrograph, fiber-fed spectrograph, echelle spectrograph, scrambler, radial velocity, exoplanets, asteroseismology

1. INTRODUCTION

High precision spectroscopic measurements have led to significant breakthroughs in the fields of exoplanets research and asteroseismology during the 13 last years. The first exoplanet 51 Peg-b was been detected in 1995 by Mayor & Queloz (1995). Thanks to improvement in Doppler measurement techniques, radial velocities have continuously increased their accuracy and offer now the possibility of detecting exoplanets in the super-earth mass domain, to measure the tiny oscillation modes of stars for probing their internal structure and to characterize the actual mass of transiting planets detected by photometry. The high stability and high optical throughput of current spectrographs also permit real progress in topics like stellar abundance analysis, rotational velocity determination, discovery of very low mass stars, stellar pulsation and activity, vertical distribution of galactic disk stars, *etc.* (Le Coroller *et al.* 2007).

In this context, and taking into account the limitations of the ELODIE spectrograph (Baranne *et al.* 1996) as well as the performance of HARPS (Mayor *et al.* 2003), we undertook to develop and build a new spectrograph called SOPHIE to be operated at the 1.93-m telescope of the Haute-Provence Observatory as a northern counterpart of HARPS. SOPHIE and HARPS scheduler and on-line data reduction software are then very similar. SOPHIE, in scientific operation since October 2006, plays a very efficient role in the follow-up of the CoRoT space mission launched in December 2006 (Baglin *et al.* 2007) by characterizing the newly discovered exoplanet candidates (Alonso *et al.* 2008; Barge *et al.* 2008).

SOPHIE was successfully used in the follow-up of the Super-WASP ground-based cameras (Cameron *et al.* 2007) and led to the unambiguous detection of p-modes on Procyon (Mosser *et al.* 2008). The major requirements for SOPHIE were to improve the over-all optical throughput by a factor of 10 and the radial velocity measurement accuracy by a factor of 2 to 3 compared to ELODIE. This permits to extend dramatically the number of observed stars while pursuing the long-term observations of the ELODIE era (since 1994).

In Section 2 we describe the instrument optical design and the technical options used to achieve the high optical throughput and high long-term stability required for high accuracy radial velocity measurements. In Section 3 we present a summary of the instrument characteristics and achieved performance. We conclude in section 4 by an overview of observed limitations and perspectives for the instrument.

2. INSTRUMENT DESCRIPTION

2.1 Guidelines

SOPHIE's architecture benefits from experience gained with ELODIE and HARPS. A cross-dispersed echelle spectrograph, which design is fully described next section, is installed in an isothermal environment. Spectra are recorded on a 4kx2k CCD cooled at -100°C . Starlight is collected at telescope focal plane and feeds the spectrograph through an optical fiber link (see section 2.3). Two observation modes are available: the High Efficiency mode (HE) and the High Resolution mode (HR), to favor high throughput or better radial velocity precision respectively. Each mode used two fibers: one for the star and the other, located 1.86 arcminutes away, for the sky spectrum or simultaneous calibration lamp exposure, the same as in ELODIE. The ELODIE bonnette (Baranne *et al.* 1996) is still used but should be replaced with an enhanced version (see section 4); it holds the calibration lamps, the atmospheric dispersion corrector and the guiding system, starlight being collected at the focal plane through a hole at center of the field mirror. This architecture has the advantage over the Iodine-cell absorption technique of using a larger wavelength range and to avoid loss of optical throughput, allowing the observation of faint stars (Pepe *et al.* 2003). Our new design leads to 1) gain on throughput by a factor of 10, 2) increased spectrograph stability by a factor of 3, and 3) increased spectral resolution (from 42000 to 75000) compared to ELODIE.

2.2 Spectrograph Description

The entire optical design is oriented to privilege long-term spectra stability and throughput as explained below. Light exiting from the fiber link (see Figure 1) is collimated by a spherical mirror and, after folding by a plane mirror, comes through the Schmidt chamber where main dispersion is achieved by the echelle grating while the cross dispersion is done with a prism in double pass. The dispersed returned collimated beams are reflected on the folding mirror and are then focused by the spherical mirror to form the image on the CCD through a field lens behind the pierced plane mirror.

The spectrograph is installed in the Coudé room of the 1.93-m telescope building, minimizing the fiber length to 17 m instead of 25 m for ELODIE. The whole instrument is mounted on shock absorbers supported by the telescope pillar structure to avoid vibration instabilities. The only moving element, the shutter with an electro-magnetic mechanism, with a fast aperture time of only 10 ms, has been cautiously damped to avoid transmission of any vibrations through the granite bench. The spectrograph thermalization is a key-point for the desired level of measurement accuracy, and a three-stage strategy was adopted. The spectrograph is installed in a thermally-controlled insulated box of $2.1 \times 0.85 \times 1.2 \text{ m}^3$ with a daily thermal stability better than 0.01°C , inside a two-stage thermalised room of $3 \times 2 \times 2 \text{ m}^3$ at 21°C . Up to 20 temperature probes are distributed around the instrument to measure variations, and one is used for fine regulation. All potential disturbing elements, CCD in its cryostat, mechanical exposure shutter and photomultiplier tube from the exposure meter, are outside the box. The automatic daily N_2 filling for CCD cooling at -100°C is done from outside the thermalised room, so that the slight effect of about 0.05° on the spectrograph lasting 2 hours disappears before observing time. This double protection also permits to completely eliminate diffuse light from observing and control rooms of the 1.93-m.

SOPHIE covers the spectral range 387 – 694 nm, for which all optical surfaces are coated: silver coating (Denton) for mirrors and antireflection coatings for all dioptrics. A new master for the ruled echelle grating was specially ordered to benefit from the first replicas, so that a grating efficiency of 80% instead of the nominal 60% has been achieved, a major point. To minimize the number of separate optical surfaces, hence increasing the mechanical stability, SOPHIE is a double-pass Schmidt echelle spectrograph, with a single mirror as collimator and focuser, a Schmidt plate corrector, the

prism and the echelle grating, a field lens in front of the detector, and a pierced folding mirror for space arrangement (see Figure 1). Large optics for a beam diameter of about 200 mm limit obstruction losses to only 15% by the folding mirror apertures and to 22% by the whole spectrograph.

Thanks to the thermal stability, no refocusing is necessary, and the spectrograph is fed by a fixed off-axis ferrule, ending the four-fiber link described next section; it is deported at 85 mm from optical axis without excessive effect on aberrations, since the four fiber terminations are concentrated inside a 500-micron diameter. The detector, an EEV CCD (4kx2k with 15 μm pixel size), is on-axis to limit field aberrations. The Schmidt plate is slightly decentered (~ 0.5 mm) relatively to the collimator axis to optimize aperture aberrations. Spot diagrams are shown in Figure 2, demonstrating that image quality is not diffraction-limited but is affected by residual coma, astigmatism and field curvature.

Apart from thermal precautions, the key-point for stability is the encapsulation of the dispersive components in a constant pressure tank sealed by the Schmidt plate. This solution stabilizes the air refractive index sensitivity to atmospheric pressure variations which could typically introduce an instrumental velocity drift of 90 m.s^{-1} per mbar change. The vacuum solution for the whole spectrograph (as HARPS) has been dropped for budget reasons. Dry Nitrogen rather than Helium was chosen, despite its increased refraction index sensitivity to temperature, to prevent leakage and favor long-term stability. No significant leakage of the overpressured tank has been actually detected after 1.5 years of operation. To avoid any gravity effect, the echelle grating lines and the cryostat are set vertical.

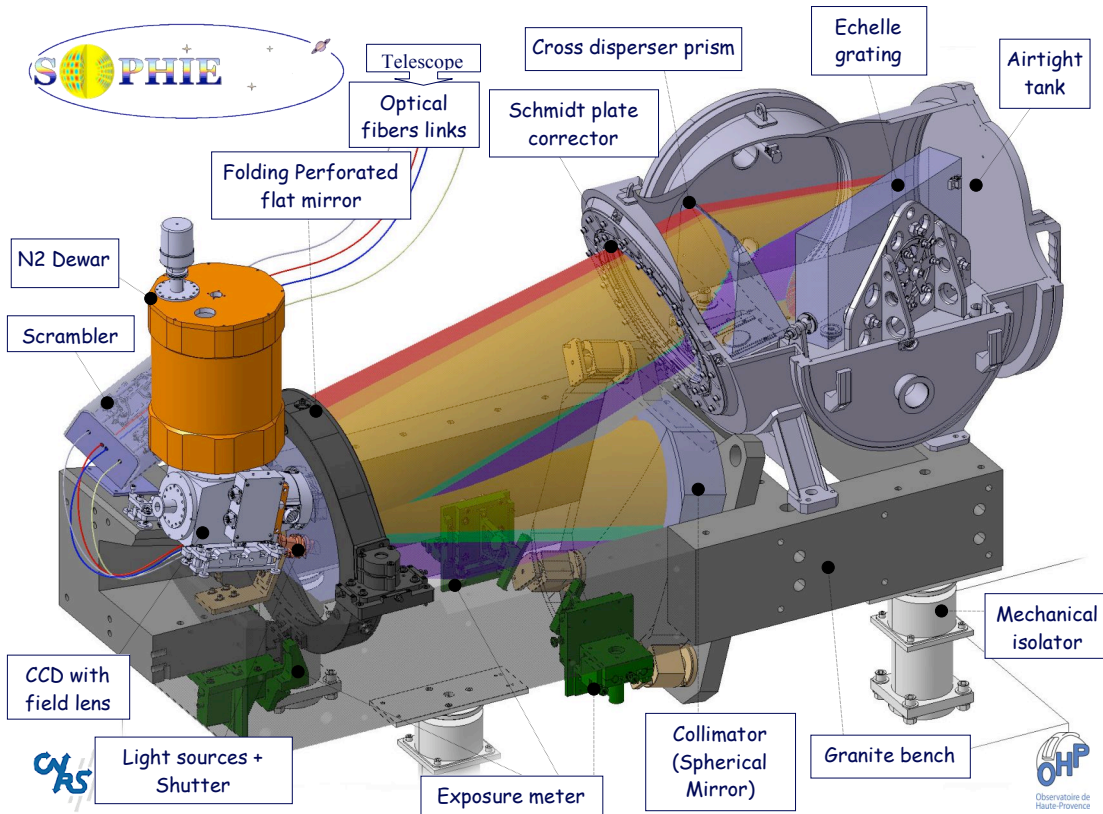


Fig. 1. The SOPHIE spectrograph, installed at the 1.93-m telescope of Haute-Provence Observatory is a double-pass Schmidt echelle spectrograph with a cross disperser, the beam being collimated and refocused by a single spherical mirror.

The main characteristics of the instrument components are listed Table 1. The echelle grating is an R2 grating ($\theta = 65^\circ$ blaze angle), manufactured by Richardson Gratings. It is a very impressive component of 240 mm x 410 mm x 74 mm, with a 52.6 gr.mm^{-1} ruled surface. The prism transmits well over the entire bandwidth, thanks to the OHARA PBL25Y glass. The combination of the echelle grating, prism, detector and focal length allows recording 39 orders for both “star” and “sky” fibers in each mode -HR or HE- from order 50 (680.6 nm to 694.4 nm, dispersion 2.25 $\text{\AA/mm} = 0.034$ \AA/pixel)

to 88 (387.2 nm to 395.5 nm, dispersion $1.27 \text{ \AA/mm} = 0.019 \text{ \AA/pixel}$). The intrinsic resolution of SOPHIE is about 200000. Fibers have a diameter of $100 \mu\text{m}$, leading to a resolution of 39 000 in HE mode, but in HR mode have an exit slit (of width $40.5 \mu\text{m}$) bonded on which increases the resolution to 75 000. Relative positions of the four fibers have been precisely adjusted; the distance between fibers of different modes ($\sim 254 \mu\text{m}$) is driven by necessary redundancy between orders, especially between red orders; the relative position of same mode fibers ($298 \pm 8 \mu\text{m}$) is driven by two constraints : having 10 background pixels between star and sky spectra and having orders spacing sufficient over the all spectrum (> 10 pixels) in order to limit order contamination; finally, fibers are disposed on a lozenge to vertically align the slit in the middle of the CCD (see Figure 3). Realization of this critical piece, called a ferrule, is described in the next section describing the fiber link.

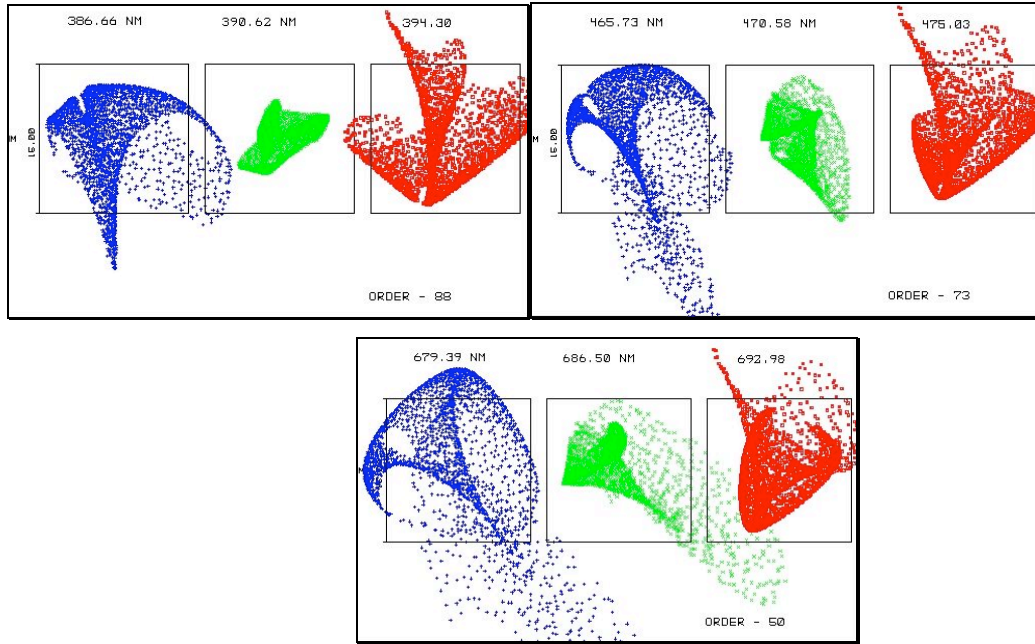


Fig. 2. SOPHIE spot diagrams for 3 diffraction orders (-88, -73 and -50). The box size is 15 microns (1 CCD pixel).

Table 1. Main characteristics of SOPHIE spectrograph components.

Component:	Characteristics:
<i>Pupil diameter</i>	Diameter 200 mm ; aperture f/3.6
Spherical mirror	Zerodur; Diameter 540 mm ; $f = 720 \text{ mm}$ (<i>Optical Surfaces Ltd</i>)
Folding mirror	Zerodur ; Diameter 440 mm (<i>Optical Surfaces Ltd</i>)
Schmidt plate corrector	BK7 ; Diameter 320 mm ; thickness 25 mm ; Kerber profile (<i>Optical Surfaces Ltd</i>)
Prism (cross-disperser)	PBL25Y ; angle 31° ; 280 mm x 220 mm ; 30 kg (<i>Optical Surfaces Ltd</i>)
Echelle grating	Zerodur ; 204 mm x 410 mm ; 52.6 gr.mm^{-1} ; blaze angle = 65° (<i>Richardson - Spectra Physics</i>)
Field lens	Silica ; diameter 90 mm ; plano-convex $R_c=245 \text{ mm}$ (<i>Optical Surfaces Ltd</i>)
CCD	EEV 44-82 ; 2048x4102 pixels ; pixel size $15 \mu\text{m}$

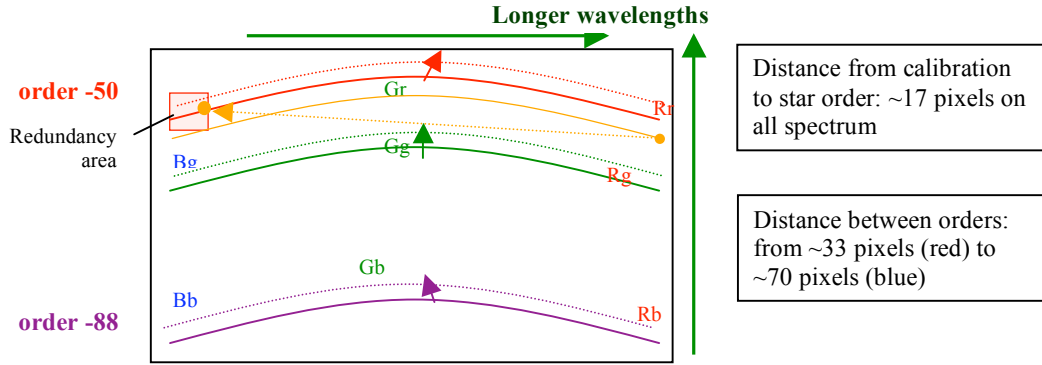


Fig. 3. Echelle spectrum configuration. Full lines: star orders; dotted lines: calibration or sky orders. B: blue, G: green, r: red. Small arrows : slit image orientation.

Straylight shielding is an important concern. Two baffles directly on the folding mirror apertures have been implemented to prevent straylight induced by the design –direct return beam through detector rectangular aperture and effects on circular entrance aperture– without impact on the wavefront. The Schmidt plate is tilted (6°) to avoid straylight coming from the collimator. Some weak ghosts are visible between orders especially for very strong Thorium/Argon emission lines, introduced by the thin ($350\text{ }\mu\text{m}$) fiber coated silica window which could not be thickened to limit spherical aberration. A mask just around the CCD effective area was carefully installed, but is sometimes insufficient for red extra-orders which produce a non-uniform diffuse background (clearly present for red stars). This is due to optical coatings being underspecified to cut red light over 695 nm .

Special care and work has been undertaken to manage the large dimensions of the optical components, especially the dispersive elements in the constant pressure tank – retractable trails were built to assure handling and precise positioning. Alignment of the ferrule was done roughly in translation, and in tilt to center the white beam on subsequent elements. Combination of grating tilts (blaze and order centering), ferrule rotation around its axis (slit orientation) and fine adjustments in translation and tilt of detector assembly, *i.e.* detector + cryostat (fine positioning in focus through astigmatic foci and centering, tilt compensation for minimizing curvature residue effect) allow to have an optimum order arrangement taking into account CCD traps and bad columns, thus avoiding star orders. This final step was done with the help of calibration lamps: tungsten for blaze optimization, and thorium for fine positioning.

2.3 Optical fiber link

Figure 4 schematically describes the fiber link that furnishes 1) ELODIE's bonnette interface, 2) aperture conversion from $f/15$ (telescope) to $f/3.6$ (spectrograph), 3) light transport from telescope focal plane to spectrograph in the Coudé room, 4) spectrograph light feed and 5) additional elements for HR mode (slit and scramblers).

The whole assembly links the moving telescope focal plane to the fixed thermalised spectrograph in the floor below, transporting star and calibration/sky flux at the Cassegrain focus from the two apertures separated by 1.86 arcminutes, through 450-micron holes in the guiding mirror corresponding to an acceptance diameter of 3 arcsec on the sky. The $f/15$ telescope aperture is converted by specially designed optics to the working aperture of both fibers and spectrograph. The star image, not the telescope pupil, is imaged on the fiber entrance, as for ELODIE. Two entrance assemblies (guiding mirror, two fibers equipped with conversion optics) are installed on the SOPHIE bonnette, and are translated on a motorized carriage to the telescope axis when a given observation mode, HE or HR mode, is chosen. The ferrule (see figure 4) terminates the link by maintaining the four fiber extremities in very precise and constant position at spectrograph entrance. The two modes differ by the addition in the HR link of two components: a $40.5\text{ }\mu\text{m}$ -width slit on the ferrule to increase spectral resolution and a scrambler to homogenize and stabilize the illumination of the spectrograph entrance despite variations due to guiding or seeing effects. The scrambler consists of two symmetrical doublets so that the image of one fiber core is the pupil for the other fiber core (Hunter *et al.* 1992).

This fiber link is crucial for the instrument's optical throughput. Several aspects are concerned. Considering the average seeing on the OHP site of 2.5 arcsec, we fixed an acceptance of 3 arcsec on the sky; compared to the ELODIE 2 arcsec apertures, this alone leads to increase average efficiency by 1.8 . Thanks to the spectrograph location in the Coudé room,

only ~17 m of fibers are necessary, limiting internal absorption. Fiber type without OH⁻ radical also reduces losses, especially in the blue region. To limit FRD (Focal Ratio Degradation) effects, a compromise is done injecting fibers at f/3.6, which is advantageous over the f/5.6 for ELODIE and f/4 for HARPS apertures by limiting flux losses. This defines also the working aperture for the spectrograph. Fresnel losses are avoided on all fiber extremities by bonding coated optics (aperture conversion optics, scrambler optics, slit window). Only two types of doublets have been ordered making both aperture conversion and scrambling optics achromatic, limiting then spectral conjugation losses. Each fiber is protected on its path from the telescope through the polar axis up to the spectrograph room by an inextensible metal hose with limited curvature. Extreme care was taken in the mounting and integration of the link.

Mechanical subassemblies and tools were all machined at Observatoire de Haute-Provence while most of the fiber link integration, mounting, bonding and control, was done in Laboratoire d'Astrophysique de Marseille clean room with the help of G. Moreaux. This has avoided dust contamination which could impact efficiency with such small optics. We use POLYMICRO FVP fibers, with a core diameter of 100 μm , FC connectors and a ferrule at spectrograph entrance. Custom fiber doublets (diameters 5 mm and 3.8 mm) were made by OPA Opticad. The slit on the coated window on the spectrograph side was produced by Optimask by microlithography with chrome.

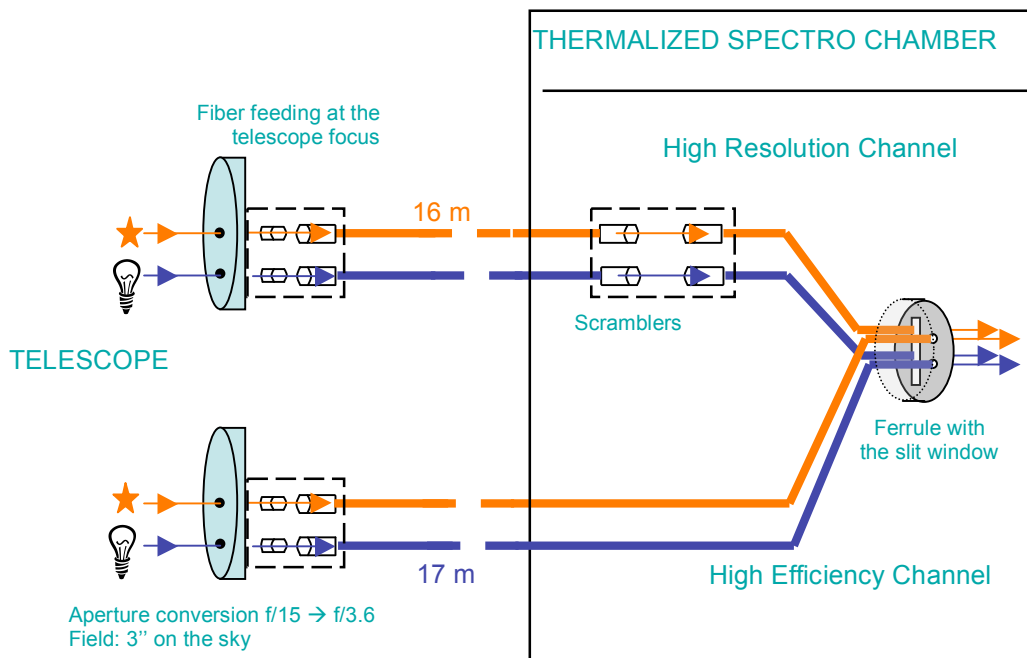


Fig. 4. Fiber link scheme.

For protection, selected fibers (on an efficiency criterion) were first individually inserted into their Witzemann hoses. Fiber extremities were bonded into FC connectors and polished allowing optical tests during all operations. Optics were bonded in their matched brass mountings with 3M C2216 and then on fiber with Polytec Epotek 301. Centering specified at 0.05 mm was optically controlled at each step. Mountings are quite complex because of their size and their multiple alignment capabilities. Entrance transfer optical assembly was aligned by construction by matching optics and mountings, whereas scrambler assembly was optimized with tilt and centering adjustment (Figure 5). Scrambler doublet alignment was verified alternatively with efficiency and exit aperture measurements (minimizing FRD).

The ferrule design, machining, building (fig. 5) and integration were one of the most critical parts of the project. More than the precision specified on exit fiber relative position, the manufacturing difficulty laid in the requirement of relative parallelism (less than 40 arcmin) to avoid vignetting and losses and exit orthogonality after polishing for homogeneity and efficiency ($\pm 1^\circ$). We managed this with a stack of 3 ferrules in RESCOR 960-HS ceramic on our conventional numerical lathe. The four 0.8mm-depth holes of the upper one were made with the same 125- μm diameter bit to assure codirectionality and relative positions of the holes. These requirements were challenging and we failed sometimes

before succeeding due to bits breakage or bits damaging leading to false holes position and direction. The other two ferrules drive the four fibers to achieve the specification (see photograph Figure 5). Integration was critical to avoid any constraints on fiber cores (simultaneously!). The ferrule stack was assembled with cyanolite glue. Then fibers were inserted in a delicate operation and bonded with 3M DP490. After polymerization, they were polished. Validation controls consisted in homogeneity, efficiency for an injection aperture of 3.6 and direction emission control. Last operation before return to telescope was the alignment (centering of the $40.5\ \mu\text{m}$ – slit onto the two High Resolution $100\ \mu\text{m}$ – core fibers) and bonding (epotek 301) of the slit window. After inserting hoses from the telescope to the SOPHIE room through the Coudé path, fiber link entrance optics were aligned (centering, tilt and depth) with respect to the guiding mirror interfaces. Finally, the ferrule has been assembled in its interface to be aligned and focused in the spectrograph as described in previous section.

The authors thank Gerardo Avila, from ESO, for his fruitful advices about the fiber link achievement.

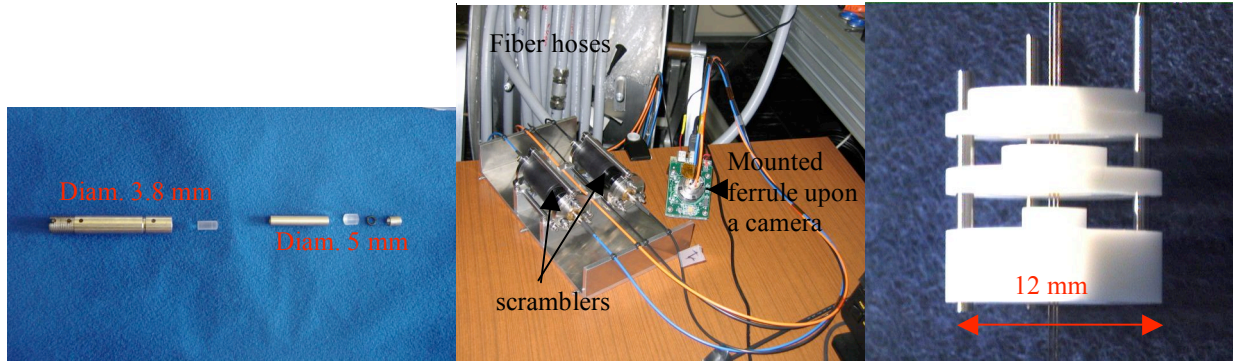


Fig. 5. Aperture conversion optics (left) – scramblers on test (center) – ferrule stack (right)

2.4 Calibration exposures - Exposure meter

The spectral calibration principle follows the HARPS and ELODIE procedure. No change has been made yet on calibration sources feeding the optical fiber link, refer to Baranne *et al.* (1996) for details. A tungsten lamp is used to locate the position of the diffraction orders and to measure the flat field. More than one thousand lines of a thorium-argon lamp are used to calibrate the spectra in wavelength with a high precision ($1\ \text{m/s}$). Each lamp can illuminate both fibers of each mode (HR or HE). Illumination of the sky-hole by the thorium-argon lamp during a stellar exposure is very useful for high precision radial velocity measurement. A shortpass rejection filter has been added in front of the lamp to avoid any background caused by wavelengths upon $694.6\ \text{nm}$. Furthermore, this calibration beam is optically attenuated in the bonnette according to the stellar flux in order to get a total thorium illumination independent of the exposure time. The sky-hole fiber can also be used to analyze simultaneously the sky background or the moonlight contamination.

An exposure meter records continuously the flux entering the spectrograph. This information is very helpful in selecting the optimum observing time, taking account atmospheric conditions. Furthermore, this allows computing the true mean time of the exposures, which is critical for accurate correction for the Earth's velocity. Note that the variation of the radial projection of the Earth's motion on the line of sight, at OHP, can be as large as $1.5\ \text{m.s}^{-1}.\text{min}^{-1}$. The exposure meter is fed by white light out of the efficient beam entering the spectrograph, a part vignettted by the grating sides. Two rectangular plane mirrors direct light with the help of the collimator to a photomultiplier outside and just below the spectrograph (Figure 6). Each mirror as pupil of the exposure meter is imaged on the photomultiplier by a doublet to make photometric measurements.

Two LEDs at $570\ \text{nm}$ are also implemented illuminating the CCD in far-field to monitor some detector long term changes as cosmetics evolution, flat field, gain and noises.

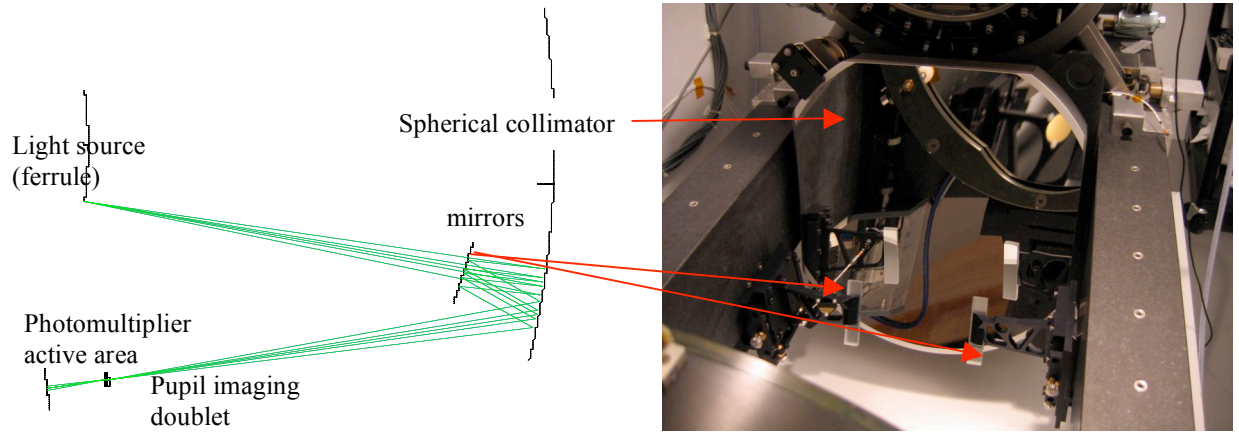


Fig. 6. Exposure meter optical layout and photograph.

3. CHARACTERISTICS AND PERFORMANCES

Table. 2. Summary of the SOPHIE instrumental characteristics.

Instrumental parameter	Value
Field on the sky	3 arcsec
Spectrograph working aperture	f/3.6
Pupil diameter	200 mm
Typical resolution power	39 000 in High Efficiency mode 75 000 in High Resolution mode
Wavelength domain	387 nm – 694 nm
Number of orders	39
Typical vertical width of the orders (90% of the energy)	7 pixels
Pixel sampling per FWHM	6.7 in HE mode 2.7 in HR mode
Detector	1 CCD EEV 2kx4k (61 x 31 mm) Pixel size 15 μ m
CCD read-out noise	6.0 e- fast mode / 2.1 e- slow mode
CCD read-out duration	19 s fast mode/ 175 s slow mode
Internal precision of the wavelength calibration	1 m/s
Observed instrumental velocity error	3-4 m/s
Efficiency at 390 nm	4.6% HE / 1.9% HR
Efficiency at 550 nm	10.4% HE / 4.3% HR
Efficiency at 690 nm	8.3% HE / 3.5% HR
(including atmosphere, telescope, Cassegrain adapter, fibers, spectrograph and CCD)	
S/N ratio per pixel at 550 nm	S/N = 100 in 1 hour on mag 11 (HE) S/N = 100 in 1 hour on mag 10 (HR)

A summary of the main SOPHIE instrumental characteristics is presented Table 2. Figures 7 and 8 show the image and the extracted spectra of 51Peg obtained with SOPHIE. Observed resolutions are 39 000 and 75 000 in HE and HR mode respectively.

During average nights at OHP with a seeing of 2.5 arcsec, in one hour exposure time, a S/N of 100 per pixel at 550 nm can be achieved for a star of $m_V = 11$ in HE mode and $m_V = 10$ in HR mode (Figure 9). This corresponds to a global optical throughput of 10.4% in HE mode and 4.3% in HR for a seeing of 2.5 arcsec, taking into account atmosphere absorption (~20%), acceptance on the sky of 3 arc-sec, telescope efficiency (~64%) , Cassegrain adapter (~97%), fiber link (~84% in HE, ~33.6% in HR) and the spectrograph (~47% at 550 nm, ~33% at 400 nm). Relative sensitivity of SOPHIE decreases in blue region (~4.6% in HE at 490 nm) due essentially to the CCD response and absorption in fibers. Such efficiency allows observing up to 15th magnitude targets which is useful for the CoRoT follow-up.

Figure 10 (left) shows the monitoring of the grating temperature sensor from December 2006 to April 2008 relatively to the average temperature of 21°C. Since October 2007 (improvement of the isolation of the thermal box) the dispersion of the temperature over long time scale is less then 0.03 deg RMS; during one night the dispersion is lower than 0.01 deg RMS. Figure 10 (right) shows the monitoring of the pressure sensor inside the airtight tank containing the dispersive optical components. The pressure variation over 1 year is less than 1 mbar. For comparison the atmospheric pressure in OHP shows variations of ± 15 mbar. When we correct the pressure sensor from the temperature variation inside the tank, we see that the pressure inside the tank is extremely stable around a slow trend, which is not yet fully explained.

This leads to a high stability of the spectra on the CCD, as shown on Figure 11, where the position of one Thorium line on the CCD since December 2006 is plotted. The spectral line has been falling systematically inside the same CCD pixel (15 micron) for 1.5 year, demonstrating the high intrinsic stability of the spectrograph. During one night the typical drift of the spectrograph, computed on an averaged of few thousands thorium lines, is less than 0.01 pixel, corresponding to about 15 m/s. This drift is monitored, thanks to the simultaneous thorium fiber, with an accuracy of about 1 m/s, as shown Figure 12. The difference between the two fibers (star and sky) is less than 1 m/s RMS.

4. CONCLUSION AND PERSPECTIVES

The SOPHIE spectrograph meets all the objectives and specifications set at the start of the program. The optical throughput of SOPHIE is better than ELODIE's by 2.5 magnitudes and the intrinsic stability is improved by a factor 10 to 20. The present radial velocity precision obtained on stable stars is about 3-4 m/s over several months. This limitation is mainly due to guiding and centering effect on the fiber entrance at the telescope focal plane. We are starting to design and develop a new Cassegrain fiber adapter including a high precision guiding system with the goal to reach the accuracy level of 1 m/s.

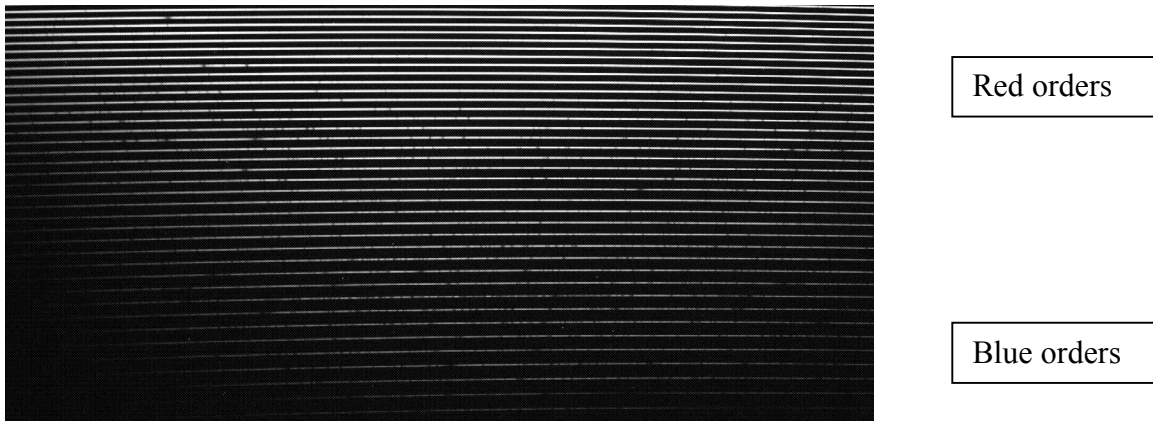


Fig. 7. Spectra of 51Peg obtained with SOPHIE - full frame (4102 x 2048) – 39 spectra orders.

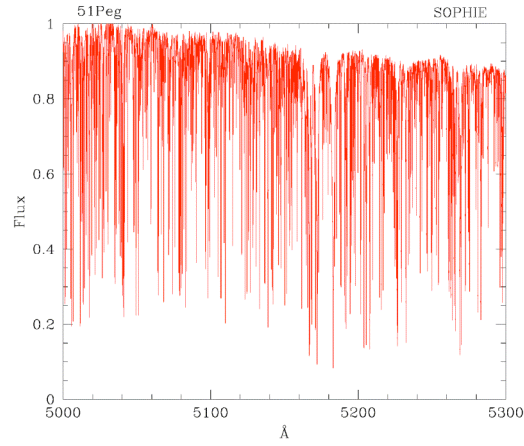


Fig. 8. Partial extracted spectra of 51Peg after calibration obtained with SOPHIE with the High Resolution Mode.

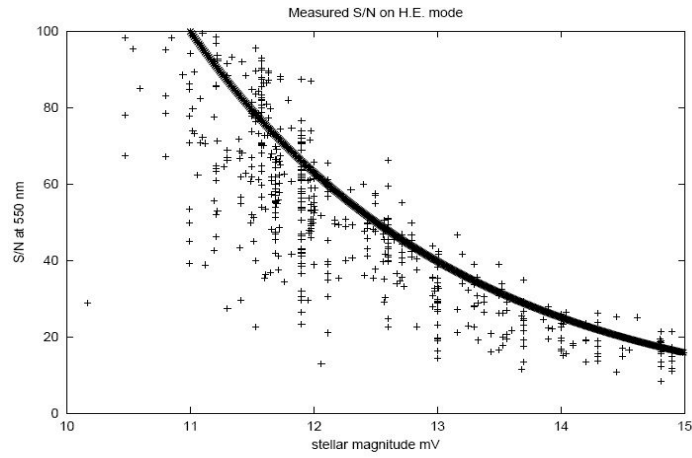


Fig. 9. Signal-to-noise per pixel at 550 nm of SOPHIE spectra obtained within the High Efficiency mode and scaled to 1 hour exposure. The black line corresponds to the expected S/N. This figure illustrates the high efficiency of the spectrograph and the fact that under good seeing condition, the S/N may be greater than expected.

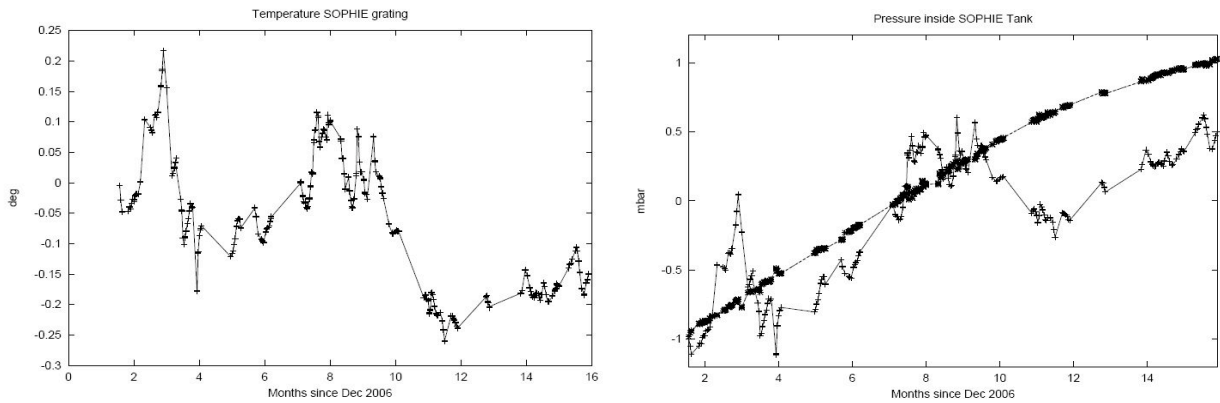


Fig. 10. From December 2006 to April 2008: (Left) Grating temperature and (Right) airtight tank pressure (superimposed trend corresponding to pressure corrected of temperature effect).

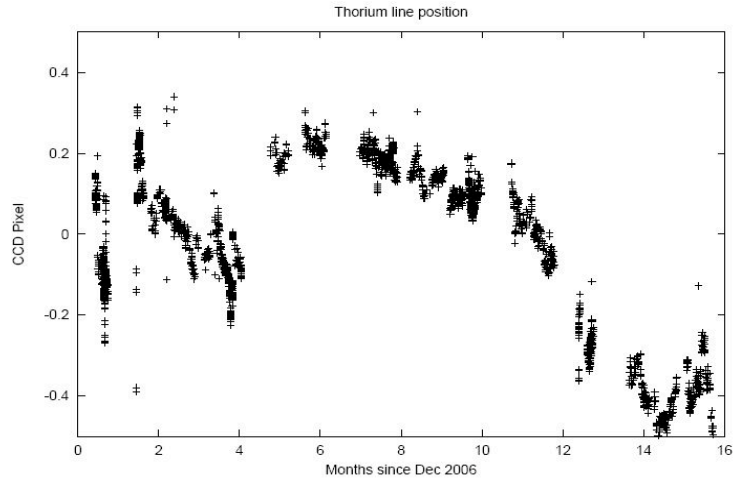


Fig. 11. One Thorium line position on CCD from December 2006 to April 2008.

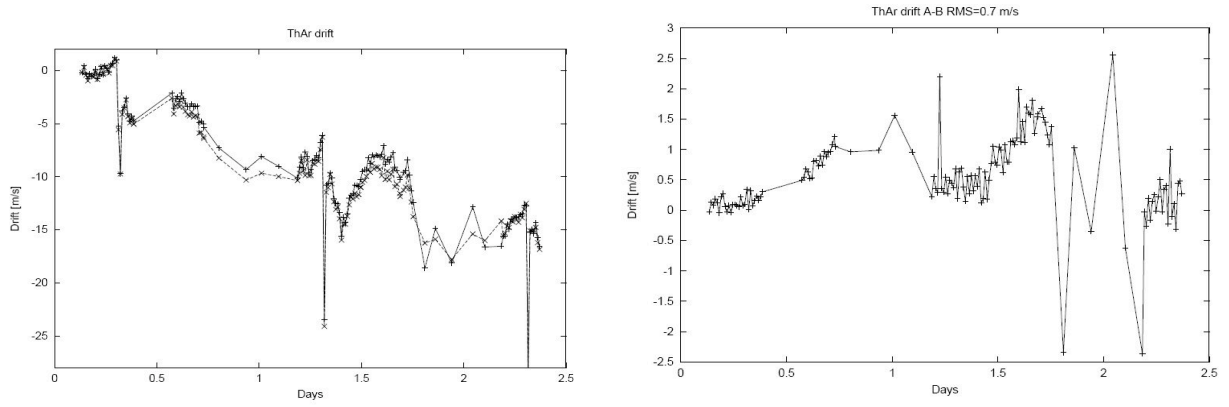


Fig. 12. Spectrograph drift during 2.5 days, monitored with the two fibers illuminated with Thorium lamp (left) and difference between the two fibers (right).

ACKNOWLEDGEMENTS

SOPHIE has been financed by the INSU (CNRS – Institut National des Sciences de l’Univers – France), the region PACA (Provence-Alpes-Côte d’Azur – France) and the OAMP (Observatoire Astronomique Marseille-Provence – France). We are thankful to these organizations for their confidence and generous support. We are grateful to the Geneva Observatory for its helpful support.

REFERENCES

- ¹ Mayor, M. and Queloz, D., “A Jupiter-Mass Companion to a Solar-Type Star”, *Nature* 378, 355 (1995)
- ² Le Coroller, H. *et al.*, “Latest News of the SOPHIE Spectrograph at Haute-Provence Observatory”, *Proc. SF2A*, in press (2007)
- ³ Baranne, A. *et al.*, “ELODIE: a spectrograph for accurate radial velocity measurements”, *A&AS* 119, 373 (1996)
- ⁴ Mayor, M., Pepe, F., Queloz, D. *et al.*, “Setting New Standards with HARPS”, *The Messenger* 114, 20 (2003)
- ⁵ Baglin, A., Auvergne, M., Barge, P. *et al.*, “The CoRoT mission and its scientific objectives”, in *Fifty Years of Romanian Astrophysics*, AIP Conference Proceedings, Vol. 895, 201 (2007)
- ⁶ Alonso, R., Auvergne, M., Baglin, A. *et al.*, “Transiting exoplanets from the CoRoT space mission. II. CoRoT-Exo-2b: a transiting planet around an active G star”, *A&A* 428, L21. (2008)
- ⁷ Barge, P., Baglin, A., Auvergne, M. *et al.*, “Transiting exoplanets from the CoRoT space mission. I. CoRoT-Exo-1b: a low-density short-period planet around a G0V star”, *A&A* 482, L17 (2008)
- ⁸ Cameron, A. C., Bouchy, F., Hébrard, G. *et al.*, “WASP-1b and WASP-2b: two new transiting exoplanets detected with SuperWASP and SOPHIE”, *MNRAS* 375, 951 (2007)
- ⁹ Mosser, B., Bouchy, F., Martiñ, M. *et al.*, “Asteroseismology of Procyon with SOPHIE”, *A&A* 478, 197 (2008)
- ¹⁰ Pepe, F., Bouchy, F., Queloz, D., Mayor, M., “From CORALIE to HARPS: Towards 1 Meter/Sec RV Precision”, in “Scientific Frontiers in Research on Extrasolar Planets”, ASP Conference Series, Vol. 294, Edited by Drake Deming and Sara Seager, 39-42 (2003)
- ¹¹ Mosser, B., Bouchy, F., Martiñ, M. *et al.*, “Asteroseismology of Procyon with SOPHIE”, *A&A* 478, 197 (2008)
- ¹² Hunter, T. R., Ramsay, L. W., “Scrambling properties of Optical Fibers and the Performances of a Double Scrambler”, *PASP* 104, 1244 (1992)